NEMESIS
Negative Effects in Medical Sciences Oral and Maxillofacial Surgery
UCL PRESSES UNIVERSITAIRES DE LOUVAIN

Medical and dental hidden treasures and secrets of 2700-year-old Egyptian mummy: Osirmose - the doorkeeper of the Temple of Re.

Authors:
Olszewski R DDS, MD, PhD, DrSc, Prof[1,2*],
Hastir JP Binf[3]
Tilleux C MS[4,5]
Delvaux L MS, PhD[4]
Danse E MD, PhD, Prof[3]

Affiliations:

[1] Department of Oral and maxillofacial surgery, Cliniques universitaires saint Luc, UCLouvain, Brussels, Belgium
[2] Oral and maxillofacial surgery research Lab, NMSK, IREC, SSS, UCLouvain, Brussels, Belgium
[3] Department of Medical Imaging, Cliniques universitaires saint Luc, UCLouvain, Brussels, Belgium
[4] Museums of Art and History, Parc du Cinquantenaire 10, Brussels, Belgium
[5] Université catholique de Louvain, Pl. Blaise Pascal 1, Louvain-la-Neuve, Belgium
*Corresponding author: Pr R. Olszewski, Department of Oral and maxillofacial surgery, Cliniques universitaires saint Luc, UCLouvain, Brussels, Begium,

phone+3227645718; fax: +3227645876; ORCID iD:orcid.org/0000-0002-2211-7731

Disclaimer: the views expressed in the submitted article are our own and not an official position of the institution or funder.

Abstract

Objective: To perform a 'virtual autopsy' on the Egyptian mummy and to study, understand, and interpret three-dimensional (3D) high-resolution computed tomography (CT) scan images of Osirmose's mummy with a multidisciplinary team composed of radiologists, archaeologists, and oral and maxillofacial surgeon.

Material and methods: We studied the Osirmose's mummy, the doorkeeper of the Temple of Re, who lived during the XXVth dynasty. His mummy belongs to the Royal Museum of Art and History (Inv. E.5889). We performed a high resolution CT scanning of Osirmose's mummy. We also 3D printed the upper maxilla of the mummy and a tooth found in the oesophagus with a clinically validated low-cost 3D printer.

Results: We confirmed the male sex of the mummy. We found the heart, aorta, and kidneys inside the mummy's body. Brain excerebration was performed through the right ethmoid bone pathway. A wood stick embedded in the dura mater tissue was found inside the skull. The orbicularis oculi muscle, internal canthus, optical nerves, and calcified eye were still present. Artificial eyes were added above the stuffing of eye globes. The skull and face were embalmed with multiple layers of inner bandages in a sophisticated manner. The wear of maxillary teeth was asymmetrical and more pronounced on the maxilla. We discovered three anomalies of the upper maxilla: 1) a rectangular hole on the palatine side of tooth n°26 (the palatine root of tooth n°26 was missing), 2) an indentation at a right angle palatine to tooth n°27, and 3) a semilunar shape of edges around the osteolytic lesion distal and palatine to tooth n°28.

Conclusions: The present study provides the first evidence of a tooth removal site, and of oral surgery procedures previously conducted in a 2700-year-old Egyptian embalmed mummy. We found traces of dental root removal, and the opening of a tooth-related osteolytic lesion before the person's death. The multidisciplinary team, the use of a high resolution 3D CT scan and a 3D-printed model of the upper maxilla helped in this discovery.

Keywords: Egyptian mummy, embalming, computer tomography, head, oral surgery, 3D printing

Introduction

Currently, the existence of tooth removal and oral surgery in Ancient Egyptian civilization is not scientifically recognized in the medical literature [1, 2]. Research on this subject usually refers to early work of major pioneers in Egyptology, such as Ruffer and Eliott Smith, who performed numerous destructive autopsies of mummies at the beginning of the 20th century [3, 4]. However, none of the early Egyptologists were dentists or oral surgeons, which could have influenced their ability to correctly interpret any potential findings in the mummies' oral cavities. In 1917, Hooton described a potential round apectomy site in one ancient Egyptian Old Kingdom Giza mandible (Peabody Museum, Harvard University, Boston, USA) [5]. Hooton's discovery was later disapproved as a round hole in the mandible was found to be natural cortical bone destruction caused by a bone cyst associated with an accessory foramen mentale (trigeminal nerve) that was present on the mandible near the same anatomical area [1]. Between the sixties and the seventies of the XXth century, a British oral surgeon, Dr. Francis Leek was part of the next generation of scientists who strongly denied the existence of oral surgery during the 4000 years of Egyptian civilization [6, 7]. However, the research performed by Dr. Leek did not include any convincing modern methodology (i.e., statistics, access to primary data or multidisciplinary team expertise). Dr. Leek claimed that there was no evidence of tooth removal among the 3000 skulls that he studied [6, 7]. The collection of ancient Egyptian skulls may not represent the ideal target group for finding evidence of tooth removal, as skulls alone cannot give information about social status (commoners or elites); or the historical time period. We hypothesized that only well-preserved ancient Egyptian mummies in their original coffins would provide any evidence of human involvement in tooth removal or in oral surgery. Previous medical literature is lacking in evidence of tooth removal in Ancient Egypt, and authors who are more modern avoid any interpretation of data even when teeth were clearly missing before the person's death [8]. The absence of proof of oral surgery became a common conviction over time in Egyptology [8, 9]. However, the absence of proof does not equate to the proof of absence. Additionally, new discoveries may occur by chance, and may require an open mind. Our multidisciplinary research team began work on the mummy of Osirmose, the doorkeeper of the Temple of Re, who lived during the XXVth dynasty (747-656 BC). His two coffins and his mummy have belonged to the Egyptian collections of the Royal Museum of Art and History, in Brussels, Belgium since 1874 (Inv. E.5889). Three-dimensional (3D) computed tomography (CT) scanning of Osirmose's mummy was part of a greater project of digitalization of Ancient Egyptian human collections of the Royal Museums of Art and History (ongoing PhD thesis in Archaeology of Mrs C. Tilleux, UCLouvain, Belgium), performed in collaboration with the Department of Medical Imaging; Cliniques universitaires saint Luc, Brussels, Belgium. After some initial

observations of 3D CT high-resolution images of Osirmose, we found a tooth in the oesophagus of the mummy. After 3D printing of the upper maxilla and of the tooth, and after finding the potential empty alveolar socket that corresponded to that tooth, we discovered that Osirmose's maxilla was holding the key to another important secret treasure of medical history.

Materials and methods

An Egyptian mummy attributed to Osirmose, the "doorkeeper of the Temple of Ra", is presently kept in the Royal Museums of Art and History (RMAH) (Brussels), Inv. E.5889. It was bequeathed at the RMAH with its two coffins (middle and inner) in 1874 by the Belgian diplomat and collector É. De Meester de Ravestein (1813-1889) [10] (Figure 1).

Fig. 1. Three coffins of Osirmose. 1. Inner coffin and the mummy (RMAH, Brussels). 2. Middle coffin (RMAH, Brussels). 3. Outer coffin (Grand Curtius Museum, Liège).

The outer coffin belongs to the Grand Curtius Museum (Liège), Inv. I/628A = Eg. 83A [10]. The three coffins of Osirmose were initially part of the private collection

of Giovanni Anastasi (1780-1860), a merchant of antiquities from Alexandria, who was also appointed Consul-General in Egypt for the Kingdom of Sweden and Norway in 1828 [10, 11]. After his death, a part of his collection was auctioned in Paris in 1857 [10, 11]. The three coffins and the mummy were purchased by Antoine Schayes (1808-1859), the first curator of RMAH [10]. Schayes's archaeological collection was sold in 1859 after his unexpected death at the age of 51 [10]. At the time of this second sale, the outer coffin belonging to Osirmose and another coffin attributed to a certain Horsiesi were inverted [10]. The middle and inner coffins of Osirmose, his mummy and the coffin of Horsiesi were then purchased by É. de Meester de Ravestein, while Osirmose's outer coffin was bought by Baron Albert d'Otreppe de Bouvette (1787-1871), the first director of the Archaeological Institute in Liège, Belgium [10]. Further, É. De Meester de Ravestein donated his three coffins and the mummy to the RMAH in 1874, and Baron d'Otreppe offered Osirmose's outer coffin to the Grand Curtius Museum in Liège in 1865 [10, 12]. The funerary assemblage of Osirmose dates from the XXVth dynasty and probably comes from the Theban necropolis [10]. These chronological and geographical estimations are based on stylistic and typological criteria [10].

Another chronological indicator is the presence of the mummy's artificial eyes [10]. False eyes are one of the major innovations of the XXIst dynasty (approximately 1069-945 BC) [10]. If this mode of embalmment was widespread during this period, it seems that the use of artificial eyes was occasionally maintained until the XXVth and XXVIth dynasties [10, 13].

Osirmose was a member of an important family of Theban priests whose collective tomb was probably discovered by the merchant and collector Giovanni Anastasi during his excavations in the 1820s [10]. The coffin, cartonnage and mummy of Osirmose's father, Padiamenet, "Chief Doorkeeper of the Domain of Ra, Chief Attendant of Ra and Chief Barber of the Domain of Ra and of the temple of Amun" [14], were in the collection of the collector and diplomat Henry Salt (1780-1827) and were sold in 1839 to the British Museum (Inv. EA.6682-6683) [10]. The mummy together with the coffins of Dismutenibtes, Osirmose's mother and Padiamenet's wife, were donated to the Oslo Museum of Cultural History by Giovanni Anastasi himself in 1826 (Inv. C.47705, C.47708) [15].

A two-dimensional radiological study was attempted on the mummy of Osirmose in 1999 [10, 16]. Based on the radiographic information on the pelvic bones Francot's study concluded that the mummy inside Osirmose's coffins was indeed a female [10, 16]. This information was again reproduced in Taylor and Antoine's book on Egyptian mummies of the British Museum in 2014 [10, 14].
After obtaining permission from the curator of the Egyptian section at the RMAH, Brussels, Belgium, a mummy was transported to our university clinic, and a 3D CT scan was performed in the Department of Medical Imaging with a multi-slice CT scanner, Brilliance ICT 256 (Philips Healthcare, Eindhoven, Netherlands) [10]. All necessary permits were obtained for the described study, which complied with all

relevant regulations. 3D CT scanning was performed in two separate sections: 1) from the skull vertex to the tibia, and 2) from the tibia to the toes. We applied the following radiological protocol: 80 keV and 140 keV, 140 mAs, slice thickness of 0.9 mm, slice increment of 0.45 mm, pitch of 0.38, field of view of 400 mm, C filter, collimation 128 x 0.625, matrix of 512 x 512, and total scan length of 1860 mm.

To better understand anatomical structures, we performed 3D printing of the upper maxilla and of the tooth found in the mummy oesophagus. The 3D CT reconstruction of the upper maxilla and of the tooth was saved in an STL file. Then, the STL file was prepared with Netfabb software (Netfabb, Lupburg, Germany), and with the 3D printer software. We used a low-cost 3D printer (Up plus 2, TierTime, Beijing) that uses fusion deposition modelling technology.
Accuracy tests and clinical validation have already been performed for this specific type of low-cost 3D printer [17]. A filament of plastic (ABS) is extruded from the head of the 3D printer and deposited layer by layer on a heated support. The head moves along the x- and y- axes, and the heat support moves along the z-axis. The cost of the 3D printer is approximately 1300 euros and the cost of 700 grams of plastic filament is approximately 35 euros. We chose the lowest slice thickness of 150 microns. The time for 3D printing of the upper maxilla (21.4 grams) was set at 3 hours and 3 minutes for 157 layers, and for the single tooth (0.3 grams) the time was 4 minutes for 76 layers. The postprocessing for this type of 3D printed model was very easy and fast (a few minutes). There were only a few layers of support material to detach from the final 3D printed model. All the 3D printed models were then painted with acrylic paint typically used by modelling hobbyists to improve the visual comprehension of anatomical structures.

Results

General description

The body represents an adult of unknown age. However, further restorations added anterior and posterior wood plates, and a wood stick inside the thoracic cage, whose edge reached under the skull and face (Figure 2). There were also multiple circles of metallic wire around the head and around the upper body of the mummy (Figures 3-5, 7, 14, 16). Arms were arranged along the body, and hands rested on the thighs (Figures 3, 4). All cervical vertebrae were present (Figure 15). Thoracic vertebrae were in a poor state of preservation (Figures 2, 5, 14). The mummy itself is covered by two layers of bandages [10]. From the initial visual examination, the deepest (inner) layer was the original bandaging, blackened with embalmer balms [10] (Figures 2, 5-11, 14-16). The outer layer was made of large bandages that seems to have been applied after a restoration [10] (Figures 2, 4, 6, 10, 15, 16).

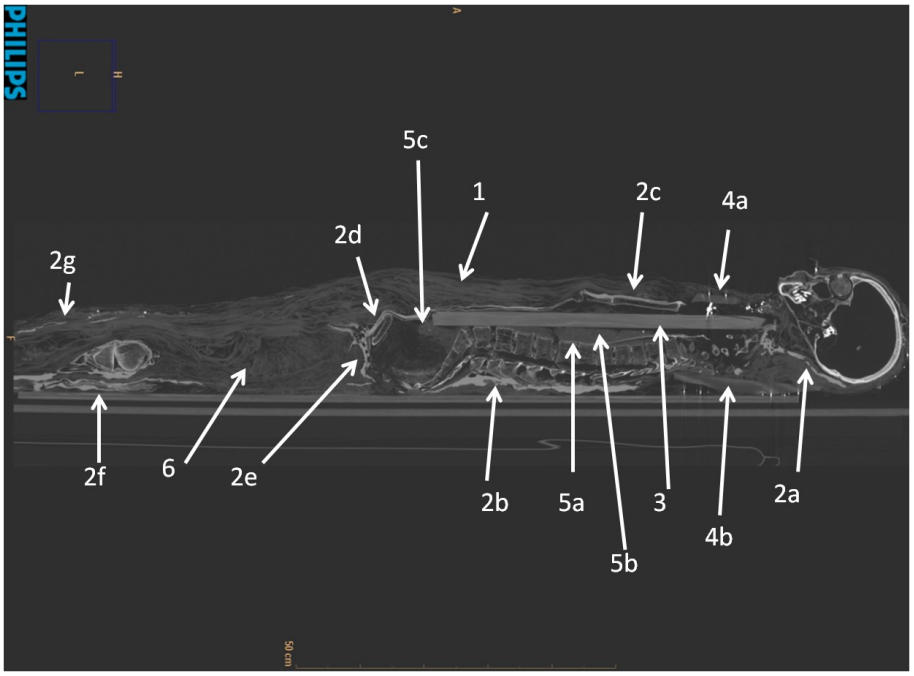

Fig. 2. General view of the 3D CT scan of the mummy from the left lateral side. 1. Outer layer of bandages at the level of the abdominal wall. 2a. Inner layer of bandages at the posterior of the skull and of the neck. 2b. Inner layer of bandages on the back of the mummy. 2c. Skin on the front of the thoracic cage. 2d. Skin in the anterior pelvic area. 2e. Skin in the perineal area and around the penis. 2f. Package of linen on the back of the left knee. 2g. Middle layer of bandages on the anterior side of the left leg. 3. Wood stick from the pelvis to the clavicle area. 4a. Anterior wood plate. 4b. Posterior wood plate. 5a. Abdominal aorta. 5b. Material of undetermined origin in the thoracic cage and in the upper abdomen. 5c. Material of undetermined origin same as 5b in the lower abdomen. 6. Layers of bandages stuffed between the thighs.

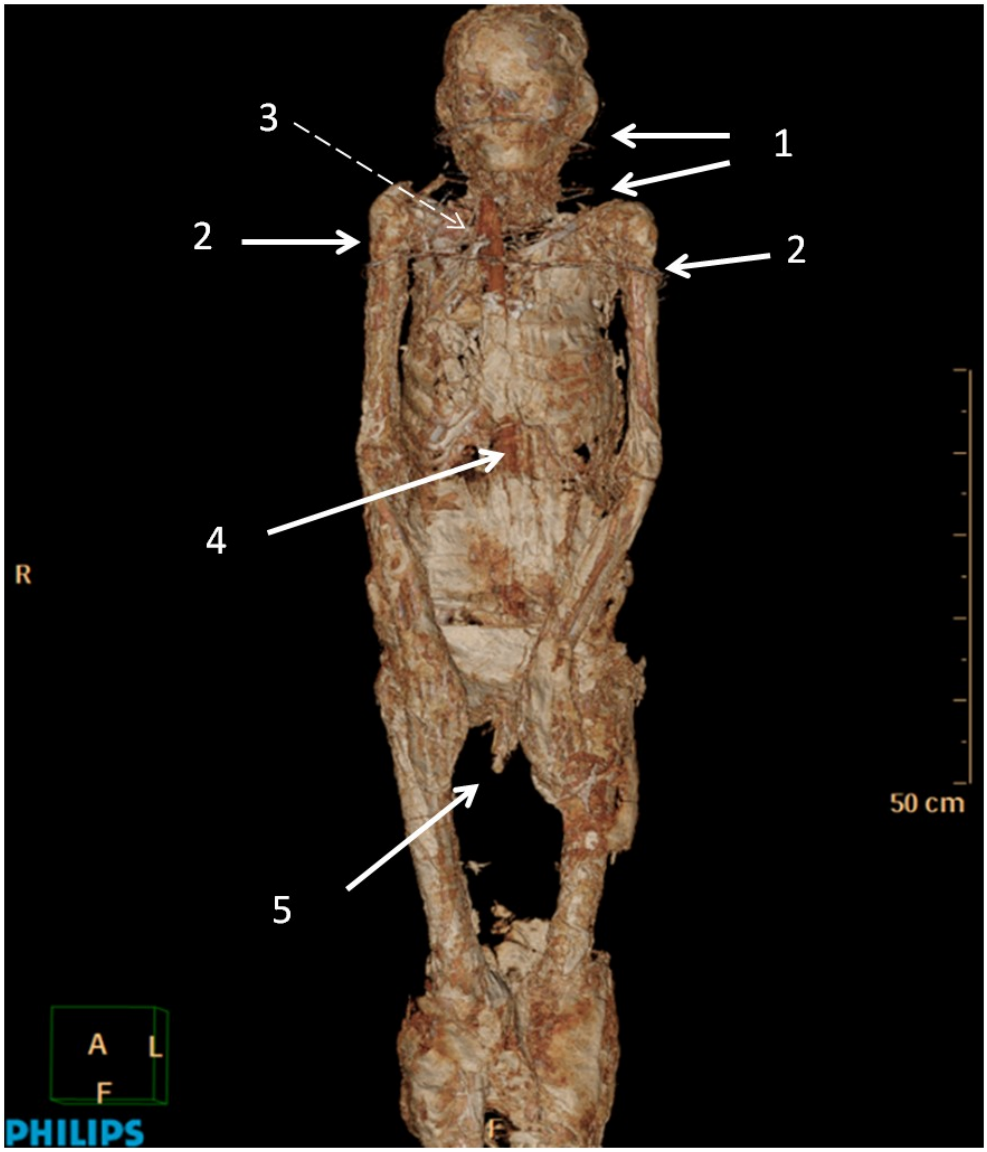

Fig. 3. 3D CT reconstruction of the mummy, anterior view. 1. Circles of metallic wire around the face and around the skull. 2. Metallic wire around the upper torso and around the upper part of both arms. 3. Dislocation of the mummy at the level of the sternoclavicular junction. 4. Wood stick oriented slightly to the right. 5. Embalmed penis.

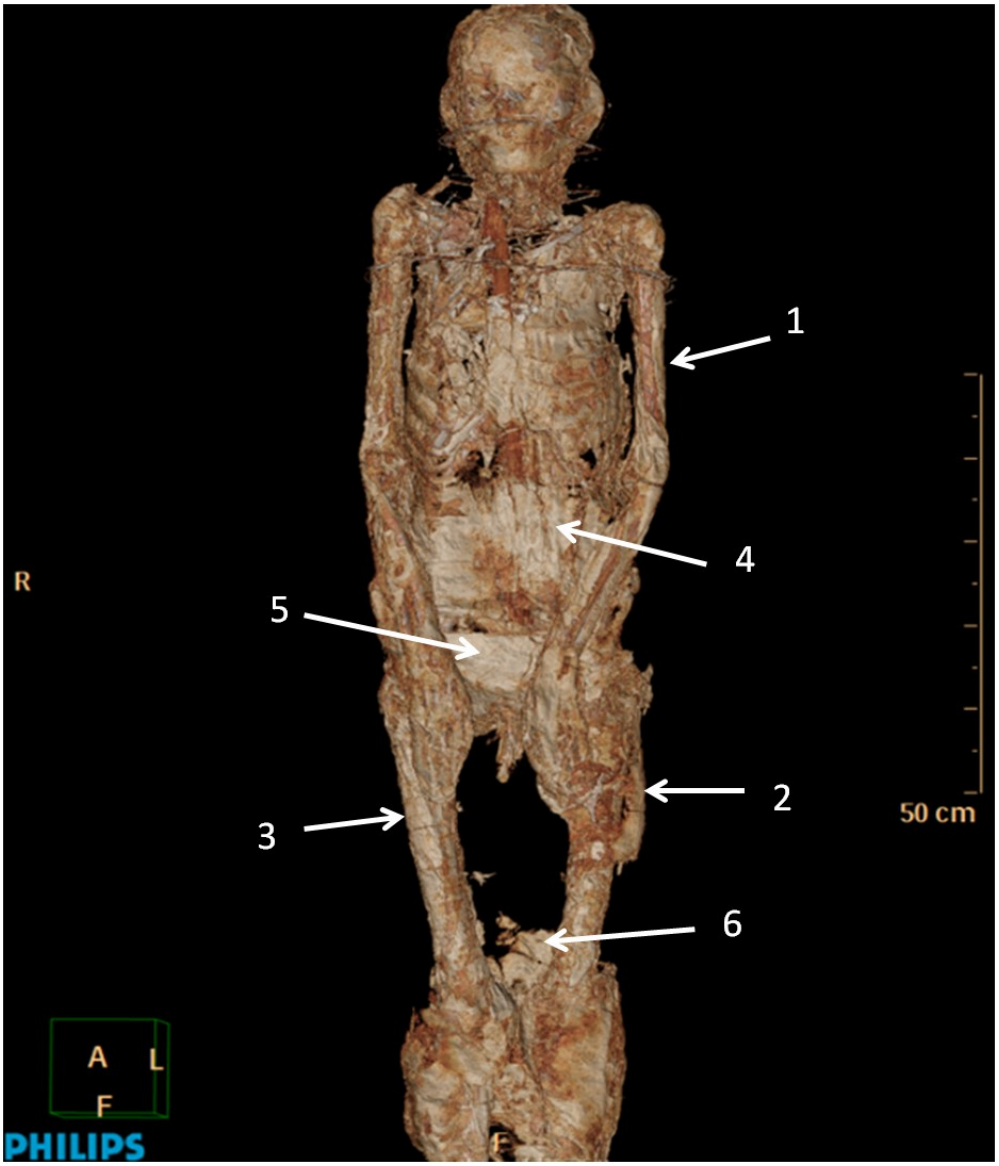

Fig. 4. 3D CT reconstruction of the mummy, anterior view. 1. Skin on the lateral side of the left arm. 2. Material of undetermined origin coated with resin on the lateral side of the left leg. 3. Skin on the lateral side of the right leg. 4. Skin on the abdominal wall. 5. Skin on the pelvic area. 6. Outer layer of bandages on the back of the legs.

239 Sex identification

240
241 The pelvic bones were broken in many places, so it was impossible to obtain sex
242 identification from the pelvis [10]. However, the sex of the mummy was identified
243 as male, as we found a well-preserved and embalmed penis on 3D CT scan [10]
244 (Figures 2-4).
245
246 Internal organs preservation
247
248 The mummified heart, cross of the aorta, and abdominal aorta were preserved in
249 the body [10] (Figures 2, 5, 6). There was a disruption of the body at the level of the
250 sternum and of the clavicle bones. A wood stick was found under the sternum, and it
251 was close to the thoracic vertebral body. The remnants of the pericardium were
252 dislodged to the right. The thoracic cavity was partially filled with radiopaque
253 substance of undetermined origin (Figures 2 (5b and 5c), 5, 6). The right and left
254 kidneys were still present in the body (Figure 5).
255

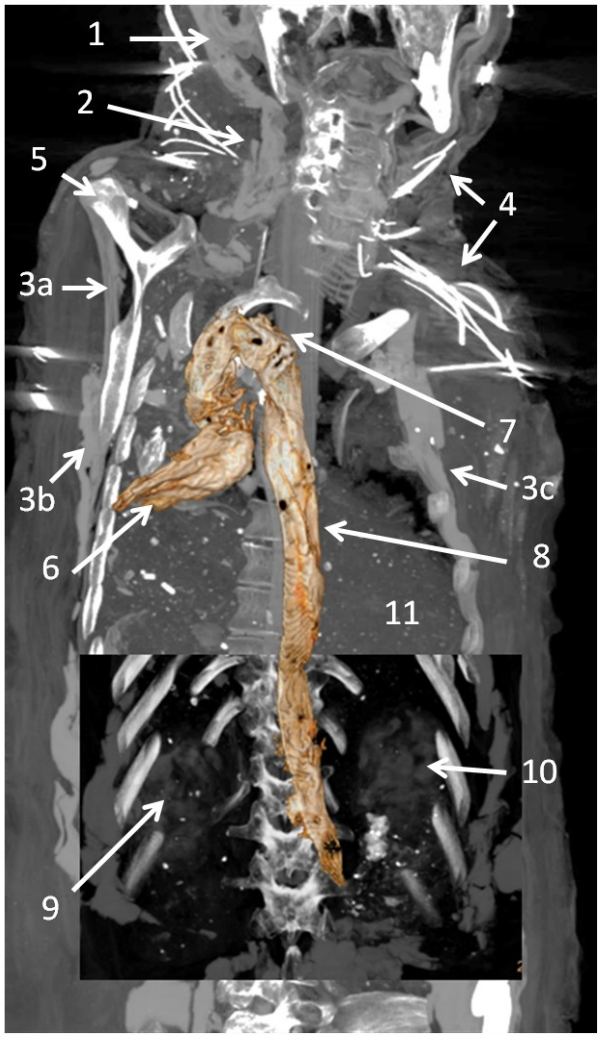

Fig. 5. 2D CT reconstruction of the neck, upper and lower thoracic cage and of the posterior abdominal area. Superimposition of the 3D reconstructed pericardium and aorta. 1. Inner layers of bandages around the right side of the face. 2. Inner layers of bandages around the right side of the neck. 3a. skin around the right side of the thoracic cage. 3b. Inner layers of the bandages around the right side of the thoracic cage. 3c. Inner layers of bandages around the left side of the thoracic cage. 4. Metallic wires from the restoration of the upper torso of the mummy. 5. Right scapula in rotation. 6. Pericardium. 7. Cross of the aorta. 8. Abdominal aorta. 9. Right kidney. 10. Left kidney. 11. Material of undetermined origin inside the thoracic cage and in the abdomen.

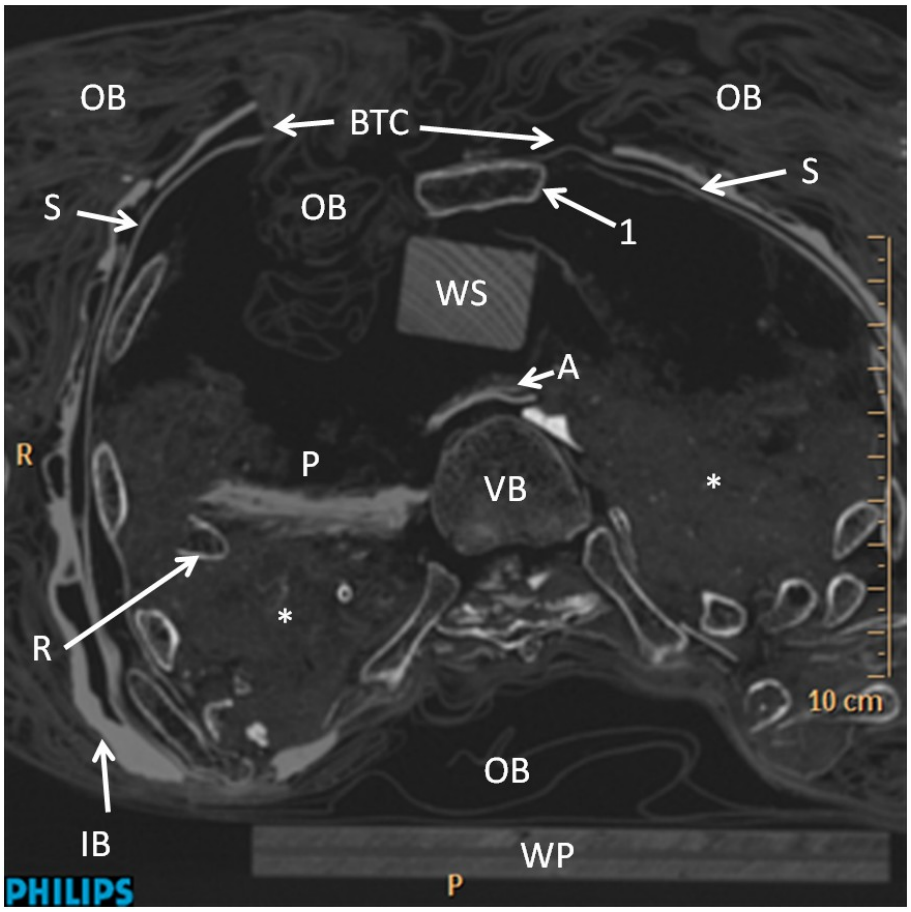

Fig. 6. 2D CT coronal view through the thoracic cage. 1. Sternum. S. Skin. IB. Inner layers of bandages. BTC. The thoracic cage was broken up and allowed with the entry of outer layers of bandages into the thoracic cage. WS. Wooden stick. P. Pericardium. A. The cross of the aorta. VB. Thoracic vertebral body. * Material of undetermined origin inside the thoracic cage. R. Rib. OB. Outer layers of bandages. WP. Main wood posterior plate.

The material of undetermined origin covers the lateral side of the pericardium (Figure 6 (*)). This means that this material was placed after the heart and aorta were replaced in the thoracic cage. The breaking of the anterior upper thoracic cage, the presence of wood stick, and the presence of outer layers of bandages inside the thoracic cage occurred after the primary embalming process, as part of a further restoration process.

Skull and face description

For the skull and face description we used a methodology already presented in our previous study on computed tomography of skulls of Ancient Egyptian mummies [18].

Brain excerebration was performed through the right ethmoid bone pathway (Figures 8, 10, 11). The nasal septum was slightly deviated to the right in the posterior area (Figures 8, 10, 11) Dura mater was found in the occipital area of the skull (Figures 13, 15, 16). A wood stick was also embedded in the dura mater tissue inside the skull [18] (Figure 13), and resin was present close to the occipital bone (Figure 13). There were no ethmoid bone fragments found on 3D CT images of the skull (Figures 13, 16). There was also a dura cervical found in the cervical spine (Figure 15). At the level of the orbits we could still recognize the orbicularis oculi muscle and internal canthus (Figure 7). Eye globes were stuffed with the material of undetermined origin (Figures 2, 8-10, 13, 14, 16). The eye remnants are present as phthisis bulbi in the posterior area of the stuffed eye globes (Figures 11, 13, 16). There were some remnants of eye muscles on the upper and on the medial sides of the stuffed eye globes (Figures 8, 10, 11). Artificial eyes in cartonage were added above the stuffed eye globes (Figures 7, 12, 13, 16). The tongue was present on the floor of the mouth which was packed with multiple pieces of linen (Figures 8, 10, 11, 15). The mouth was closed (Figures 12, 15). Pieces of linen were present over the upper and the lower lip (Figure 15 (5a), (5b)). The submandibular area was packed with a piece of linen (Figure 15, (5c)). The skull and face were embalmed with multiple layers of inner bandages in sophisticated manner (Figures 7-11, 14-16). The nasal plugs were absent. Ears were also embalmed (Figure 16).

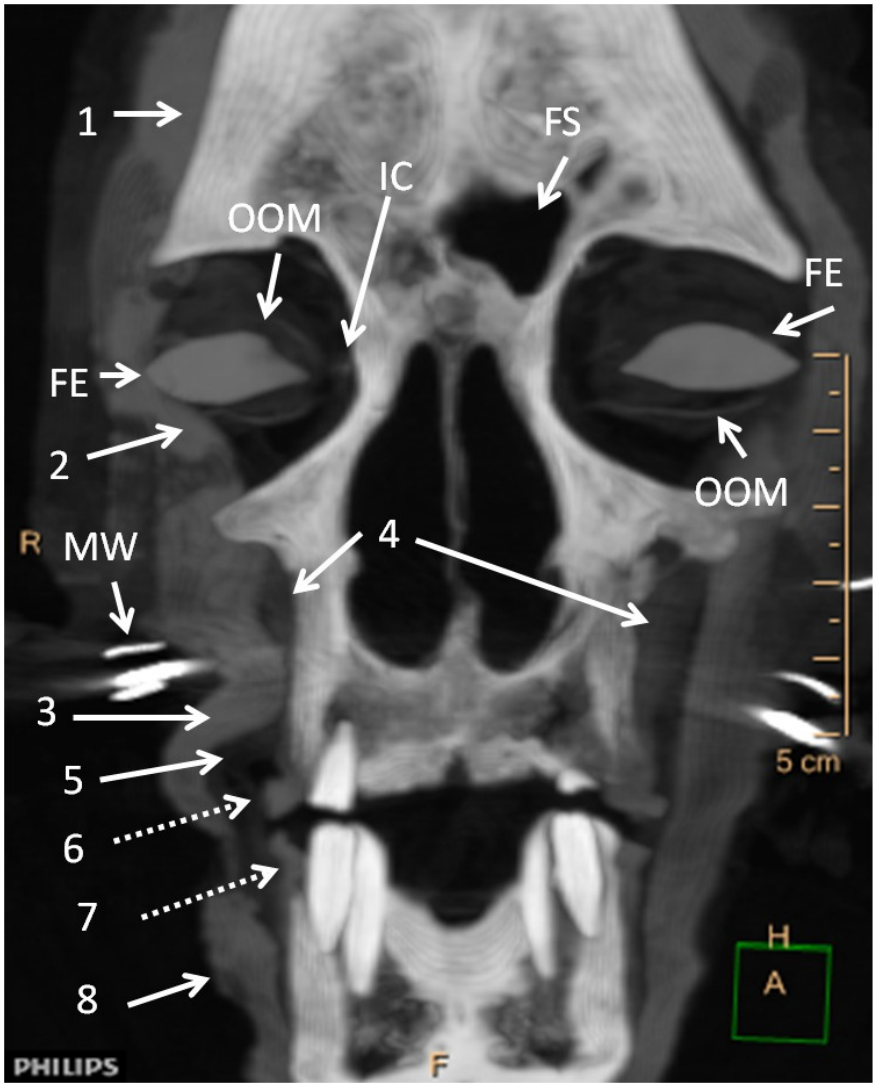

Fig. 7. 2D CT frontal and anterior view of the face and of the skull of the mummy. FS. Left frontal sinus. FE: False eye, right and left. IC. Internal canthus of the right orbit. OOM. Eylid and orbicularis oculi muscle, right and left. MW. Metallic wires. 1. Inner layer of bandages around the right frontal bone. 2. Inner layer of bandages around the right eye globe. 3. Inner layer of bandages around the right upper lips. 4. Skin. 5. Linen around the right upper lip. 6. Upper lip. 7. Lower lip. 8. Inner layer of bandages around the right mandible.

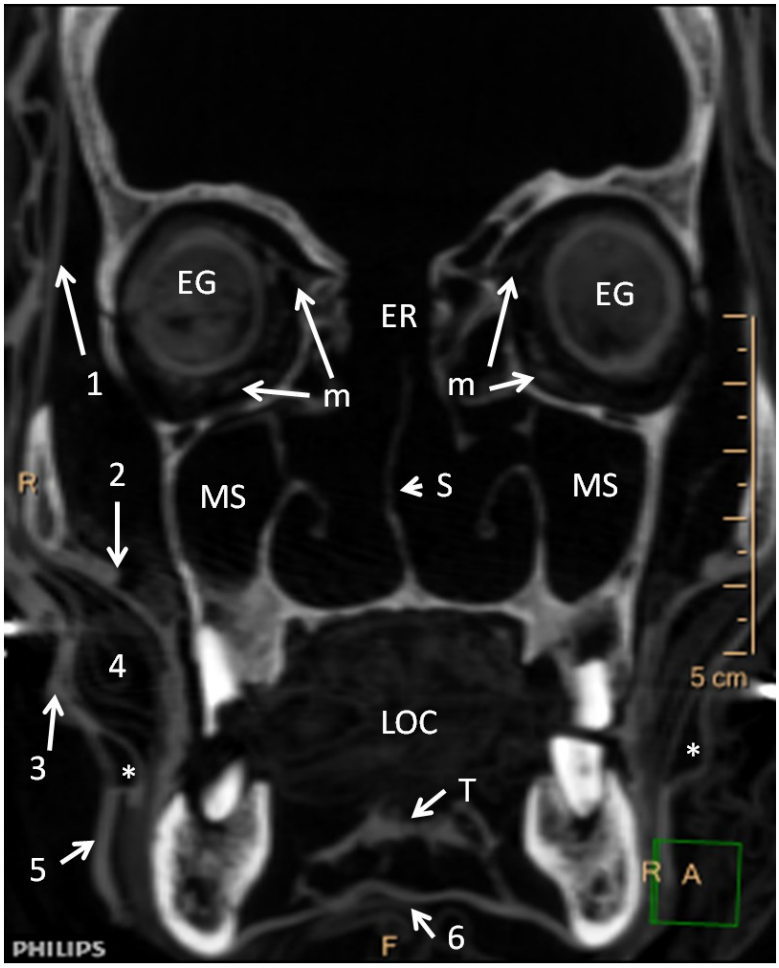

Fig. 8. 2D CT coronal view of the skull and face. EG. Eye globe stuffed with the material of undertermined origin. m. Remnants of eye muscles. ER. Excerebration road through the right ethmoid bone. S. Nasal septum slightly deviated to the right. MS. Maxillary sinus right and left, without alveolar maxillary bone pneumatisation. LOC. Linen inside the oral cavity. T. Tongue. 1. Skin of the right frontozygomatic area. 2. Skin of the right zygomaticomaxillary area. 3. Inner layer of bandages in the right zygomaticomaxillary area. 4. Linen at the level of the right cheek. 5. Inner layer of bandage around the mandible. 6. Skin of the floor of the mouth.
*: double layer in the inner layer of bandages on the right and left side of the oral cavity, and at the level of the occlusal plane.

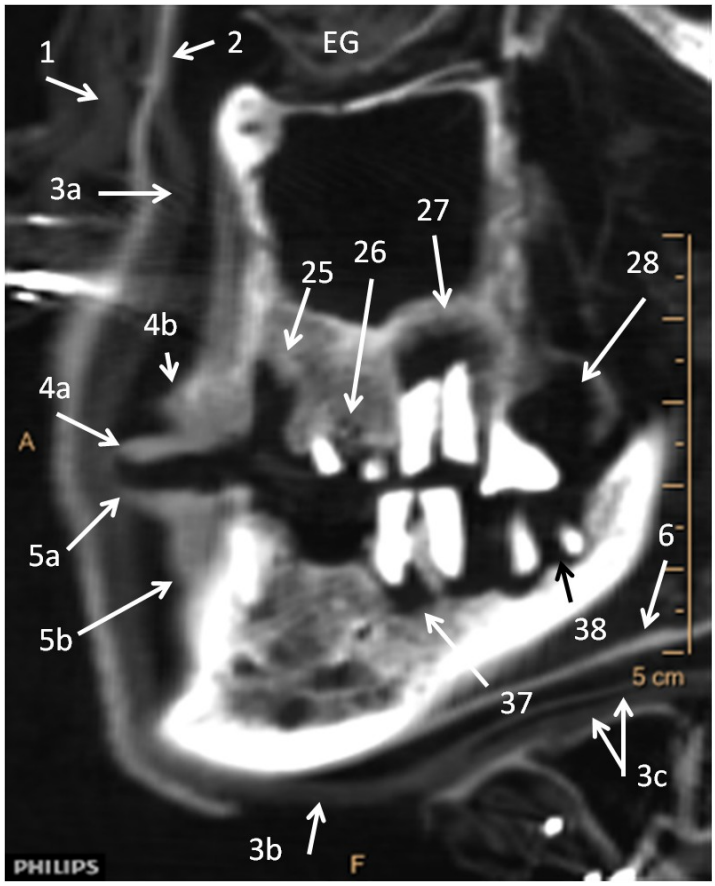

Fig. 9. 2D CT sagittal view of the left side of the face. EG. Left eye globe stuffed with the material of undertermined origin. 1. Outer layer of bandages. 2. Inner layer of bandages. 3a. Deeper inner layer of bandages around the anterior maxilla and the anterior mandible. 3b. Deeper inner layer of bandages under the anterior mandible. 3c. Double layer of the deeper inner layer of bandages under the posterior mandible. 4a. Skin of the upper lip. 4b. Skin over the anterior maxilla. 5a. Skin of the lower lip. 5b. Skin of the anterior mandible area. 6. Skin of the horizontal body of the mandible.
Tooth 25: empty alveolar socket of tooth n°25 containing initially two roots. Tooth 26: mesiovestibular and distovestibular roots of tooth n°26. Tooth n°27: osteolytic chronic lesion around the mesiovestibular and distovestibular roots of tooth n°27. Tooth n°28: osteolytic lesion distal to tooth n°28, and opened to the oral cavity. Tooth n°37: osteolytic lesion around the mesial root of tooth n°37. Periodontal disease around the distal root of tooth n°37. Tooth n°38: terminal periodontal disease around the mesial and distal roots of tooth n°38.

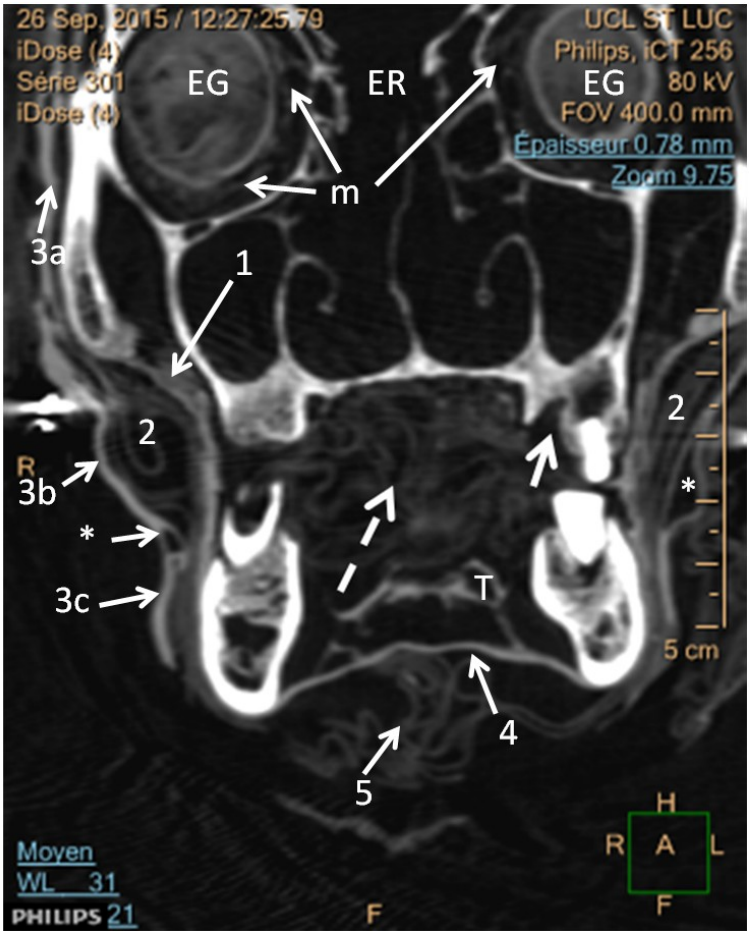

Fig. 10. 2D CT frontal view of the mummy's face. EG. eye globes stuffed with the material of undertermined origin. m. Remnants of eye muscles. ER. Excerebration road. T. Tongue. Arrow: empty alveolar cavity for palatine root of tooth n°26. Dashed arrow: a piece of linen inside the oral cavity. 1. Skin of the right zygomaticomaxillary area. 2. Linen between the skin and the inner layer of bandages at the level of the right and left cheek. 3a. Inner layer of bandages at the level of the right frontozygomatic area. 3b. Inner layer of bandages at the level of the cheeks. 3c. Inner layer of bandages at the level of the mandible. 4. Skin at the level of the floor of the mouth. 5. Outer layer of bandages under the oral cavity. *: double layer in the inner layer of the bandage on the right and left side of the oral cavity, and at the level of the oclusal plane on the left side.

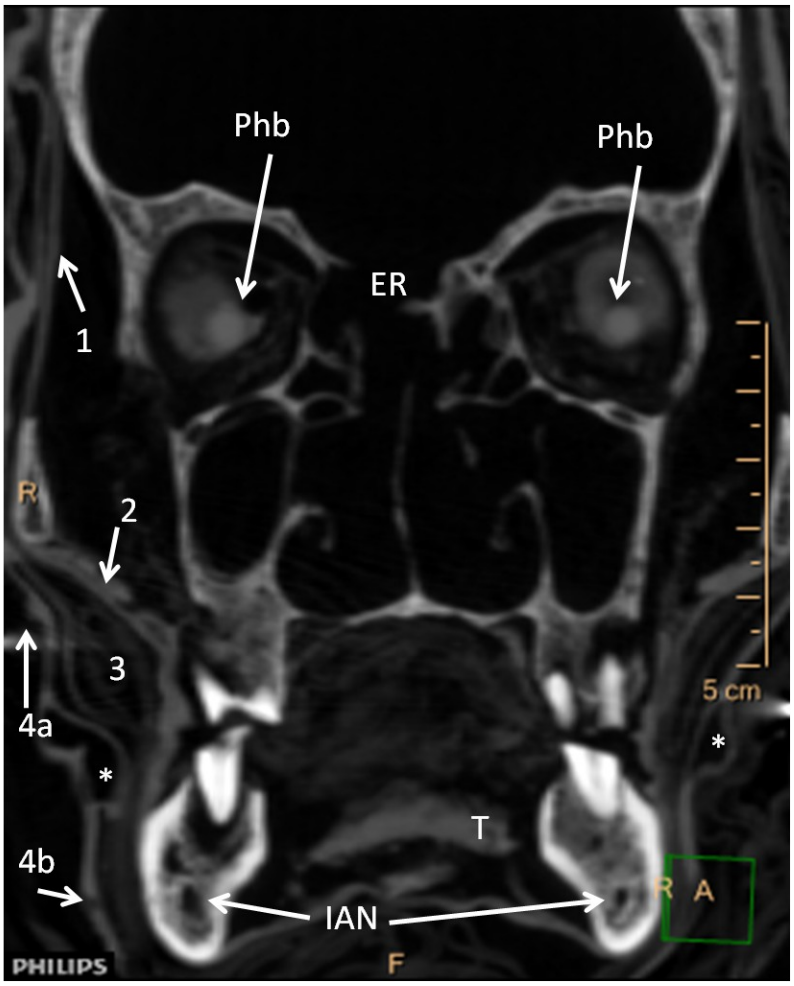

Fig. 11. 2D CT frontal view of the mummy's face. Phb. Phthisis bulbi in the posterior area of the stuffed eye globes. ER: Excerebration road through the right ethmoid bone. 1. Skin of the right frontozygomatic area. 2. Skin of the zygomaticomaxillary area. 3. Linen between the skin and the inner layer of bandages at the level of the right cheek. 4a. Inner layer of bandages at the level of the cheeks. 4b. Inner layer of bandages at the level of the mandible. *: double layer in the inner layer of the bandage on the right and left side of the oral cavity, and at the level of the oclusal plane on the right and left side. T. Tongue. IAN. Well corticalized canal of the right and left inferior alveolar nerve.

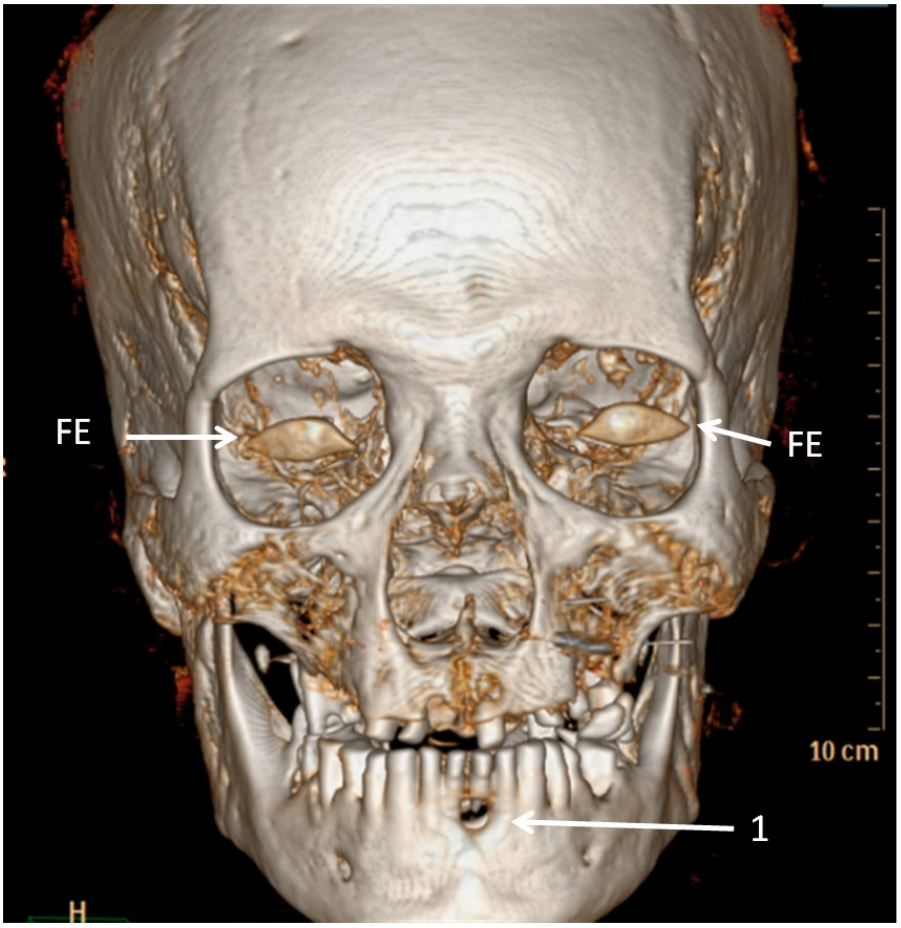

Fig. 12. 3D CT reconstruction of the head and skull of the mummy. Frontal view. Bone reconstruction. FE. False eye (cartonage). The skull and face have no fractures. 1. Osteolytic lesion around the root of tooth n°31 with perforation of the vestibular and of the lingual cortical bone.

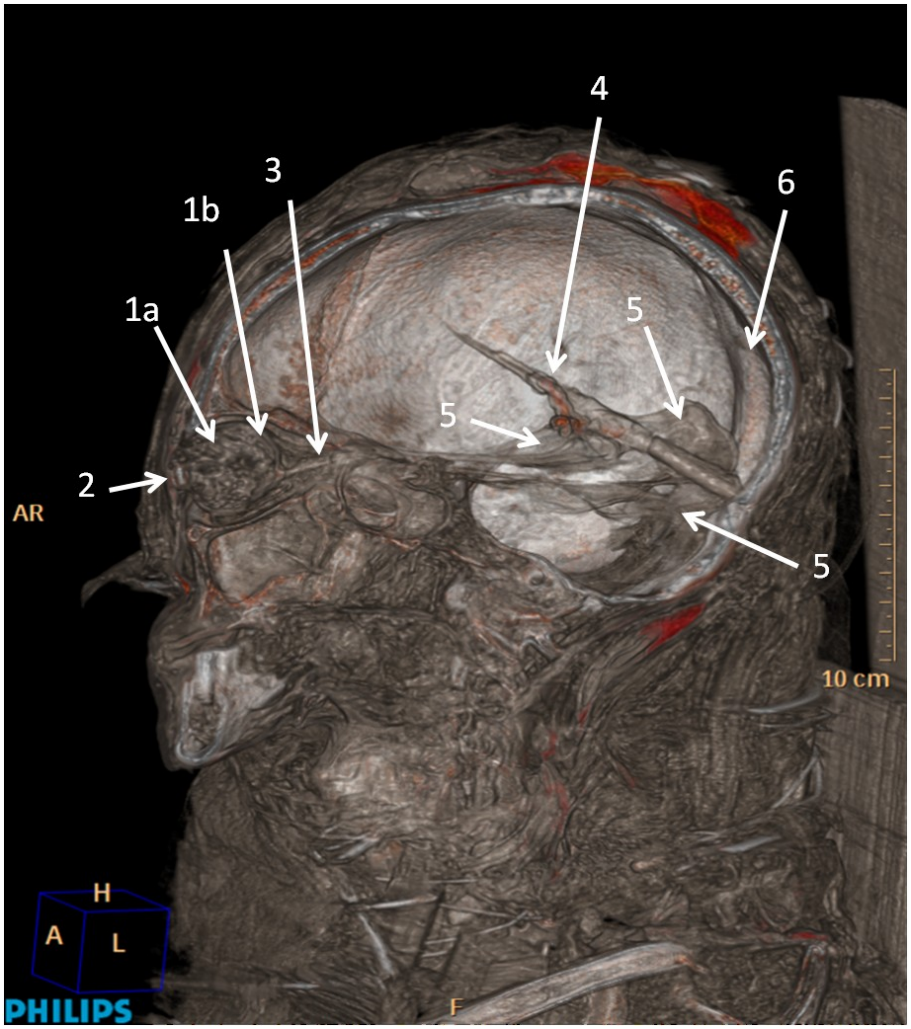

Fig. 13. 3D CT reconstruction of the head and neck of the mummy, and showing the inside of the skull. Lateral view. 1a. Stuffing of the eye globe. 1b. Phthisis bulbi. 2. False eye (cartonage). 3. Intact optic nerve. 4. Stick embedded in dura mater inside the skull. 5. Layers of dura mater. 6. Resin layer in the back of the skull against the occipital bone.

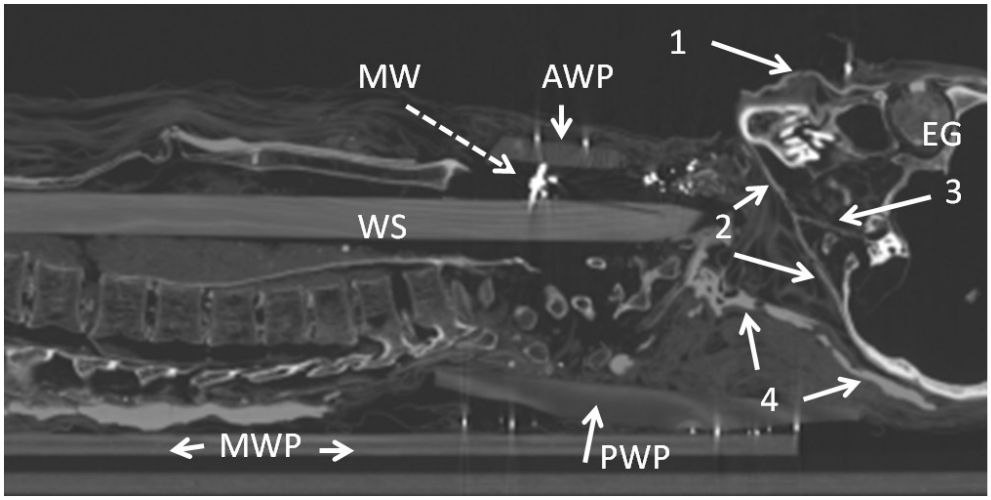

Fig. 14. 2D CT general view of the mummy. Lateral view. MWP. Main wood plate. WS. Wood stick. AWP. Anterior wood plate. PWP. Posterior wood plate. MW. Metallic wire node under the AWP. EG. Stuffed eye globe. 1. Inner layer of bandages around the face. 2. Skin under the body of the mandible up to the occipital bone. 3. Skin along the vertical ramus of the mandible. 4. Inner layer of bandages around the back of the skull and the back of the neck area.

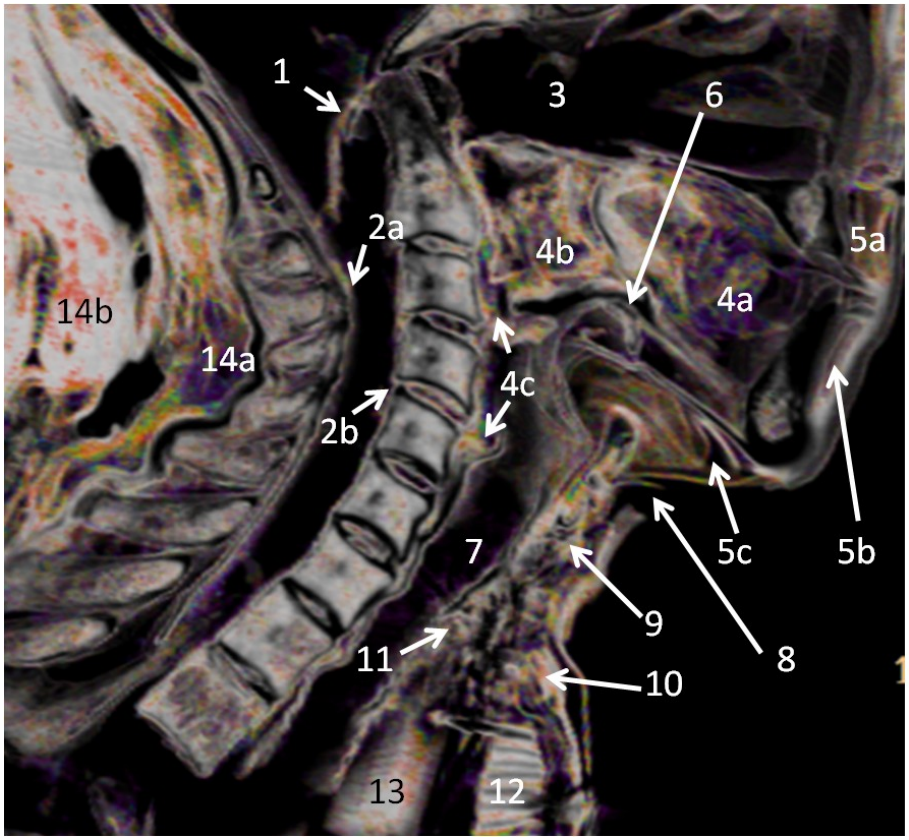

Fig. 15. 3D CT midsagittal view of the face and the neck. 1. Dura mater inside the skull. 2a. Posterior cervical dura. 2b. Anterior cervical dura. 3. Empty nasal cavity. 4a. The anterior oral cavity was filled with a piece of linen; the mouth was closed, and the linen was disposed between the front teeth. 4b. Posterior oral cavity filled with a piece of linen. 4c. Piece of linen in oesophagus. 5a. A piece of linen filling the subnasale area. 5b. A piece of linen filling the supramentale area. 5c. A piece of linen filling the submandibular area. 6. The tongue. 7. Trachea. 8. Discontinuity in the skin in the upper cervical area under the mandible. 9. A piece of linen filling the upper cervical area. 10. A piece of linen filling the anterior and lower cervical area. 11. A piece of linen filling the posterior and lower cervical area. 12. Additional piece of wood. 13. Wood stick. 14a. Inner layers of bandages in the posterior neck area. 14b. Outer layers of bandages in the posterior neck area.

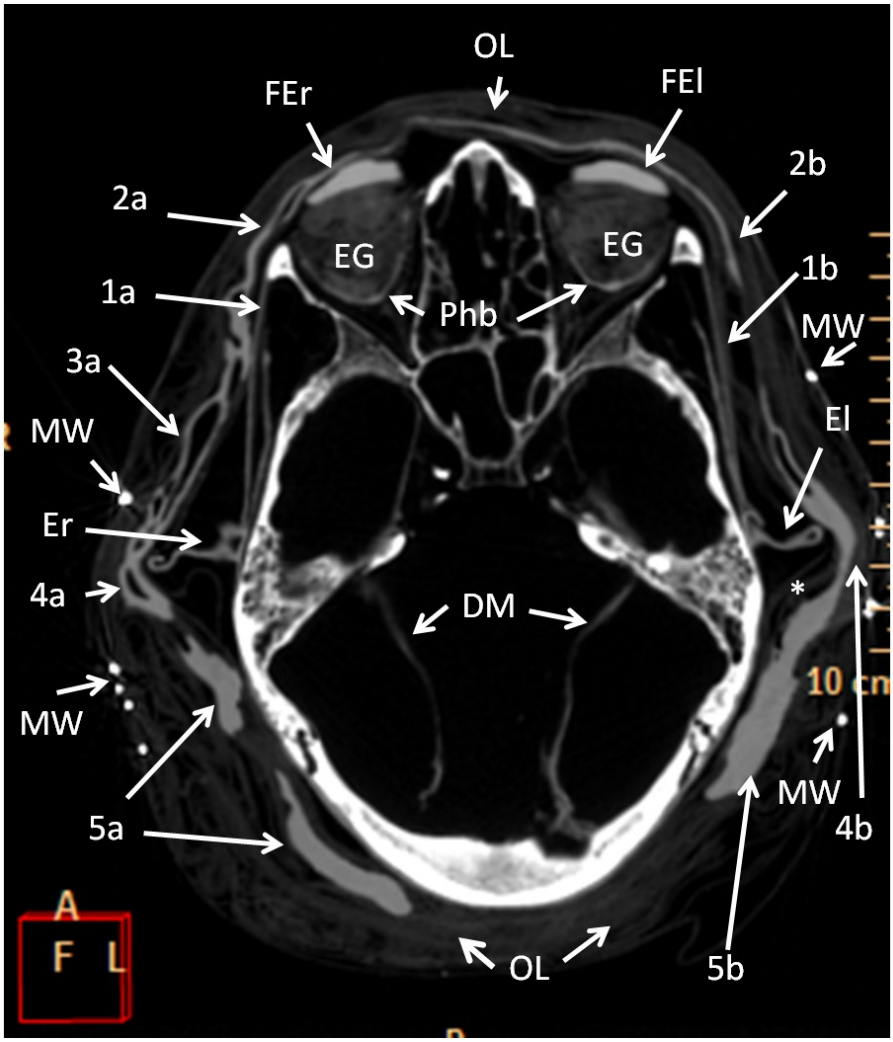

Fig. 16. 2D CT axial view of the mummy's face and skull. FEr. False eye left. FEr. False eye right. OL. Outer layers of bandages. EG. Stuffing of eye globes. Phb. Phthisis bulbi. DM. Dura mater inside the skull. MW. Metallic wires around the head. Er. Ear right. El. Ear left. 1a. Skin in the right temporal area. 1b. Skin in the left temporal area. 2a. Inner layer of bandages around the right orbit. 2b. Inner layer of bandages around the left orbit. 3a. Inner layer of bandages in the right temporal area. 4a. Inner layers of bandages around the right ear. 4b. Inner layers of bandages around the left ear. * A piece of linen around the left ear. 5a. Inner layer of bandages in the right parietal and occipital area. 5b. Inner layer of bandages in the left parietal and occipital area.

Dental status

The right and left sides of the maxillary dental arch were easily recognizable as the incisive canal opening was clearly present on the palatine midline of the upper maxilla in the 3D printed model (black arrow) (Figure 17).

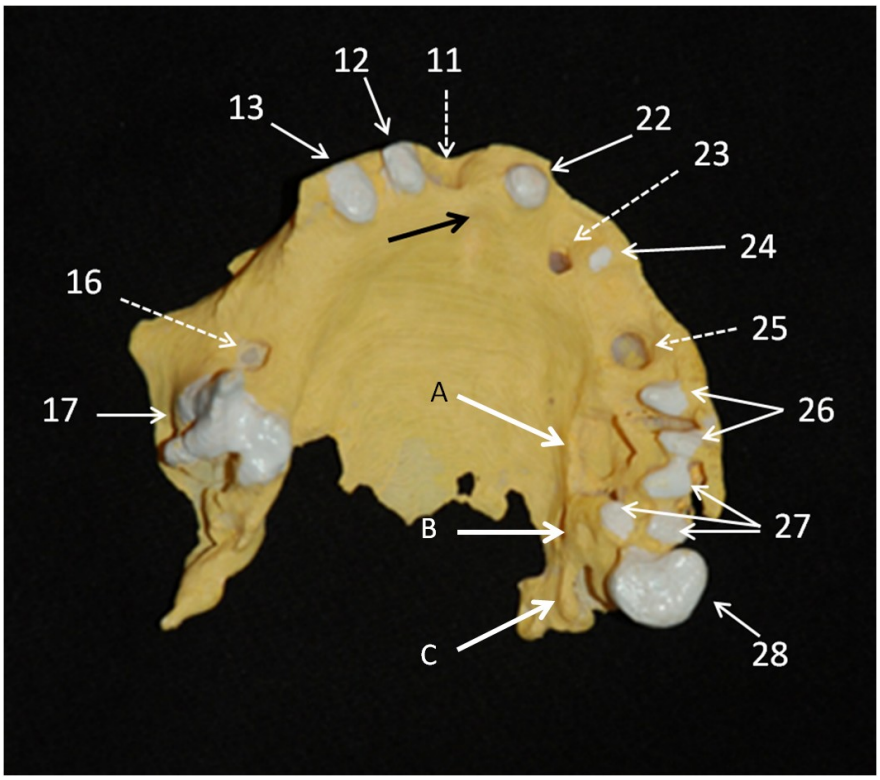

Fig. 17. Three-dimensional printed model of the upper maxilla. Superior view of the dental arch and of the hard palate. The remaining teeth were painted white, whereas the bone was painted yellow. The black arrow indicates the incisive canal on the midline. White arrows indicate teeth that are still present, and dashed arrows indicate empty alveolar sockets. The numbering of teeth follows the International Dental Federation's system. A. Artificial hole on the palatine side of tooth n°26. B. Artificial bone indentation on the palatine side of tooth n°27. C. Artificial opening of bone osteolytic lesion on the palatine and distal side of tooth n°28.

The upper maxilla and the mandible presented with multiple dental lesions (Figures 18, 19).

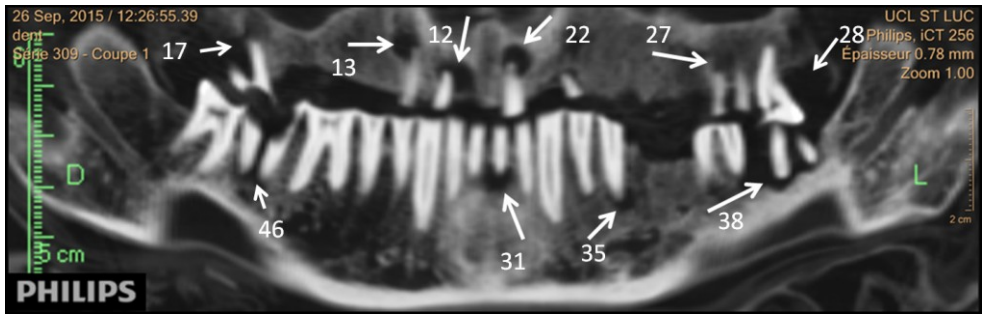

Fig. 18. 2D CT pseudo-panoramic view of the dentition. Tooth n°12: osteolytic lesion around the root of tooth n°12. Tooth n°13: osteolytic lesion around the root of tooth n°13. Tooth n°17: periodontal disease around roots of tooth n°17. Tooth n°22: osteolytic lesion around the root of tooth n°22. Tooth n°27: osteolytic lesion around the mesial root of tooth n°27. Tooth n°28: osteolytic lesion distal to tooth n°28. Tooth n°31: osteolytic lesion around the root of tooth n°31. Tooth n°35: osteolytic lesion around the root of tooth n°35. Tooth n°38: periodontal disease around mesial and distal roots of tooth n°38. Tooth n°46: rarefying osteitis around apices of mesial and distal roots of tooth n°46.

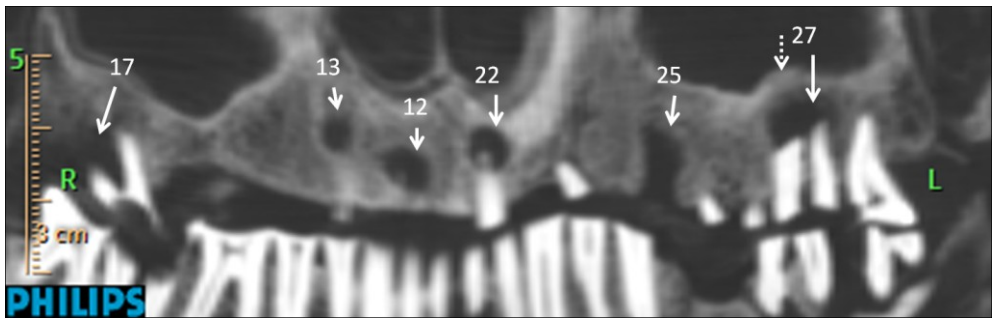

Fig. 19. 2D CT pseudo-panoramic view of the dentition. Tooth n°12: osteolytic lesion around the root of tooth n°12. Tooth n°13: osteolytic lesion around the root of tooth n°13. Tooth n°17: periodontal disease around roots of tooth n°17. Tooth n°22: osteolytic lesion around the root of tooth n°22. Tooth n°25: tooth socket with imprint of two roots at the level of absent tooth n°25. Tooth n°27: osteolytic lesion around the mesial and distal roots of tooth n°27. Dotted arrow: expansion of the lesion inside the left maxillary sinus floor.

On the upper maxilla, some teeth were still present, including the right lateral incisor (n°12), the right canine (n°13), the right second molar (n°17), the left lateral incisor (n°22), the left first premolar (n°24), and the first (n°26), second (n°27), and third left molars (n°28) (Figure 17). All of these teeth presented with major abrasion of their crowns, which is a common finding in Ancient Egyptian mummies [9]. Three open alveolar sockets existed at the level of the first right incisor (n°11), the left canine (n°23), and the left second premolar (n°25) (Figure 17). The left central incisor (n°21), the first (n°14) and second right premolar (n°15), and the third right molar (n°18) were absent from the upper maxilla. Only the left first molar (n°36) was absent from the mandible (Figure 18).
We also found a tooth left in the oesophagus with an abrased crown, and two roots (one longer and one shorter) (Figure 20).

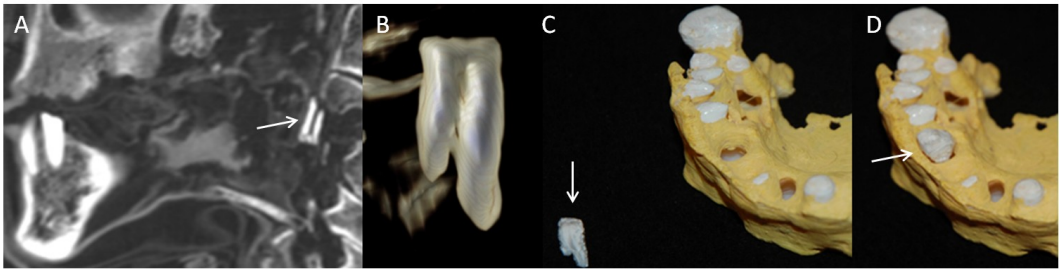

Fig. 20. Tooth found in the oesophagus. A. Two-dimensional image of the tooth and of the surrounding area. B. Three-dimensional reconstruction of the tooth with an abrased crown and broken roots. C. Three-dimensional printed tooth and 3D model of the upper maxilla. D. The second left premolar (n°25) in place again.

The 3D printed the tooth was found in the oesophagus. We checked its anatomical position in relation to the existing open alveolar sockets. There were no empty alveolar sockets in the mandible. We concluded that the tooth was a second left premolar (n°25). There were also resorbed alveolar sockets at the level of the first right molar (n°16), and first left premolar (n°24). Multiple teeth presented with apical lesions (Figures 18, 19). The creation of apical osteolytic lesions is related to the opening of dental pulp by abrasion phenomena, pulp necrosis, and bacterial migration from an abrased crown pulp chamber, through the root canal to the tooth apex, and to the bone. The shape of bony osteolytic lesions can be spherical, oval, or multilobular [19]. Figure 19 shows the apical lesion on the maxilla at the level of the lateral right incisor (n°12), the right canine (n°13), the left lateral incisor (n°22), and the first left molar (n°26). The developing osteolytic lesion may have slowly eroded the surrounding bone; and may have created an opening through the cortical bone on either the vestibular and/or the palatine side. The vestibular side was eroded in the first place (Figure 21) as it is less thick than the palatine cortical bone (Figure 23). Larger openings in cortical bones (OCs) indicate a longer period during which a lesion progressed in the living patients. Smaller openings in cortical bones (RCs)

indicate a shorter period during which a lesion progressed in the living patients (Figure 21).

Such lesions are present on the 3D upper maxilla model at the level of the second right molar (n°17), and on the first (n°26), second (n°27) and third left molars (n°28) (Figure 21). We can also see the apical lesion perforating the vestibular bone at the level of the third right molar (n°18) which is missing from the dental arch (Figure 21).

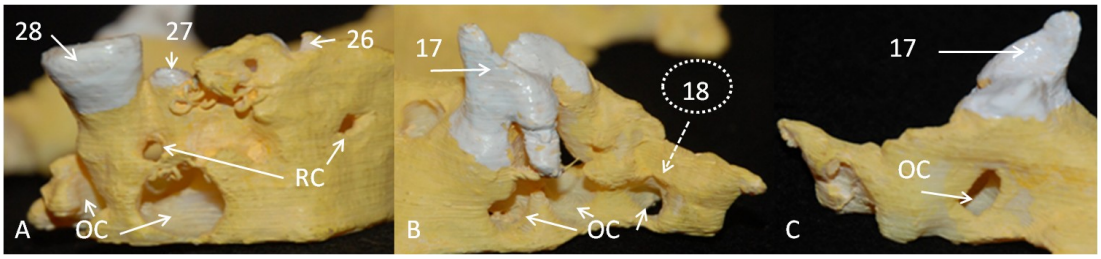

Fig. 21. Three-dimensional printed model of the upper maxilla. Apical lesions perforating the vestibular and palatine sides of the upper maxilla. A. Vestibular side lesions related to teeth n°28, n°27, and n°26. OC: Older cavity. RC: Recent cavity. B. Vestibular lesions related to teeth n°17 and to missing tooth, n°18. C. Palatine lesion related to tooth n°17. OC: Older cavity. RC: Recent cavity.

The second right molar (n°17) presented with egression, which is a slow downward movement of a tooth, bone, and surrounding mucosa that occurs during a patient's life to reach specific occlusal contact with the lower second right molar (n°47) (Figure 22). The tooth n°17 is therefore misaligned with the bony lesions it had created.

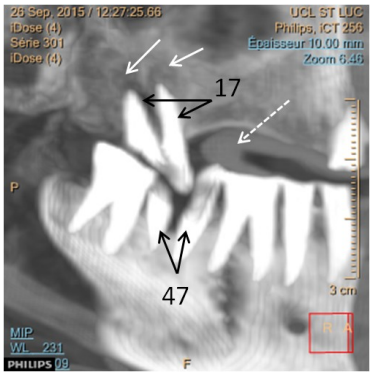

Fig. 22. Superior second right molar (n°17) in egression, with specific occlusal contact with the inferior second right molar (n°47). Arrows show bone lesions around the apex of tooth n°17. The dashed arrow shows the linen packed inside the mouth as part of the embalming process.

The growing bone osteolytic lesions that are close together may present more complex 3D shapes as they can fuse together over time. Here, we can see in the 3D printed model that bone lesion cavities are all fused together between the remaining two vestibular roots of the first left molar (n°26), the three roots of the second left molar (n°27), and the third left molar (n°28), which has only one main root (Figure 23).

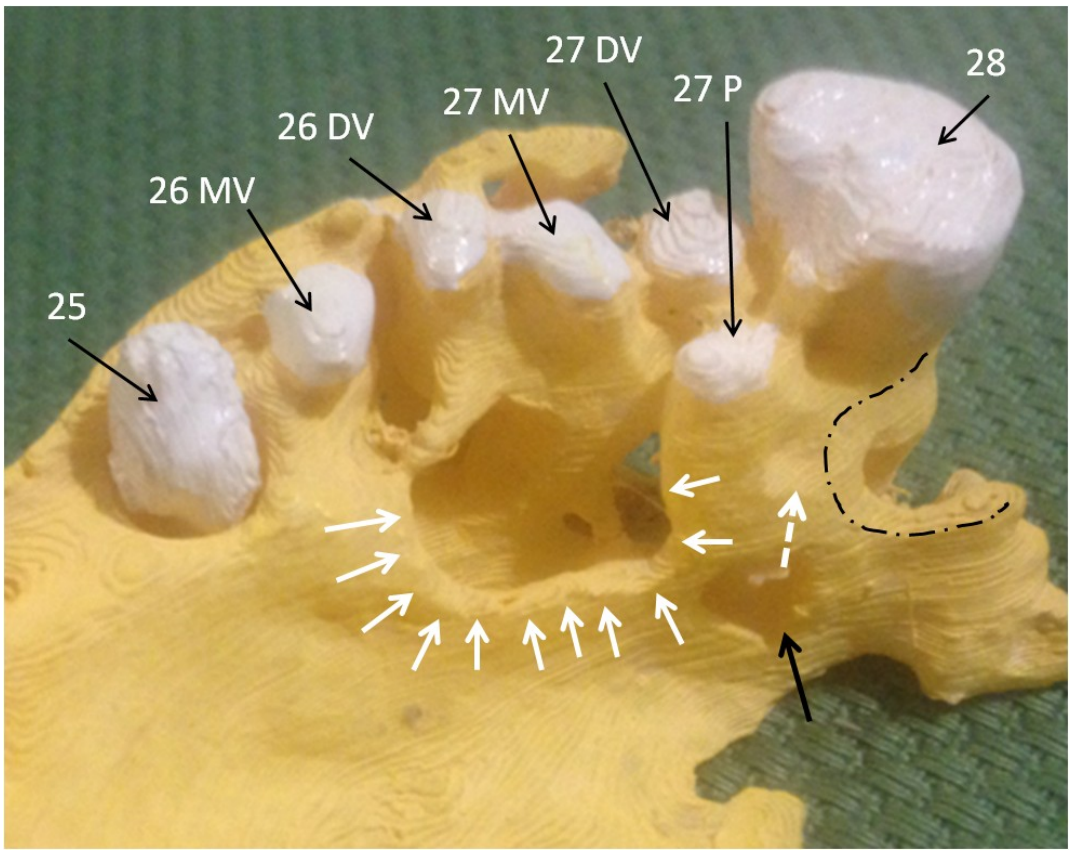

Fig. 23. Three-dimensional printed model of the upper maxilla. View from the palatine side of the second left premolar (n°25), the first (n°26), the second (n°27), and the third left molars (n°28). MV: mesiovestibular root. DV: distovestibular root. P: palatine root. At the level of the missing palatine root of tooth n°26 there is a missing bone box with straight angles (white arrows). The old osteolytic lesion opens at the level of the palatine root apex of the left second molar (n°27) (black arrow). The presence of bone indentation with straight angles on the palatine side of the palatine root of the second left molar (n°27) (white dashed arrow). Anteroposterior and oblique bone loss at the level of the palatine side of the third left molar (n°28) (black dashed line).

The palatine root of the first left molar (n°26) is missing on the 3D printed model of the upper maxilla, as it is missing on the 3D CT scan (Figures 17, 23). However, it was once present, as we can still see its massive alveolar shape as depicted in Figure 10.

The 3D-printed model of the upper maxilla also shows numerous unusual elements (Figures 17, 23):

1) rectangular box of missing cortical bone at the palatine side at the level of the missing palatine root of the first left molar (n°26);

2) bone indentation on the palatine side of the palatine root of the second left molar (n°27); and

3) anteroposterior, curved, semilunar, and oblique bone loss at the level of the distal and palatine side of the third left molar (n°28) (Figures 17, 23, 24).

The bone box space at the level of missing palatine root of the first left molar (n°26) presents with straight angles, which never occurs in natural bone lesion evolution [19] (Figures 17, 23). The box measures 9 mm and presents with an artificial shape. The edges have smoothed as the bone had time to heal, which means that the lesion appeared before the death of Osirmose.

The bone indentation at the level of the palatine side of the palatine root of the second left molar (n°27) does not corresponds to any anatomical variation nor to any pathological modification of the maxillary bone in this area (Figures 17, 23).

Bone loss at the palatine and distal side of the third left molar (n°28) corresponds to the opening of the "floor" of the osteolytic lesion, which is present around tooth n°28. The "ceiling" of the lesion is related to the apex of the tooth (Figures 17, 23, 24). The 3D printed model shows a tunnel which links older osteolytic lesions at the apex of the third left molar (n°28) and the second left molars (n°27), and presents with a cortical round palatine bone opening (black arrow) (Figure 23). The presence of bone loss on the distal and palatine side of the third left molar (n°28) does not correspond to the natural evolution of bone osteolytic lesion that perforate the cortical bone at the level of the apical tooth area.

Discussion

The example of the history related to Osirmose's mummy shows us the complexity of studying, understanding, and interpreting traces and clues left by the Egyptian civilization. Osirmose's mummy as well as the mummies of his father and mother travelled to Europe as they were part of international trade related to Egyptomania followed by Napoleon's Egyptian campaign [20]. Furthermore, Osirmose's mummy went through the turmoil of the initial creation of Egyptian collections in European museums with mistakes such as inversion of sarcophagi between mummies [10]. The body of Osirmose's mummy was also restored in modern times, adding further complexity to the endeavour to understand its anatomy. The sex of Osirmose was obscured for decades due to misinterpretation of

X-ray imaging performed in the 1990s [16], and due to further dissemination of this error through a textbook by renowned Egyptologists [14]. With a help of multidisciplinary team, we have reasserted the male sex of Osirmose's mummy (Figures 2-4). Although the heart is the central organ in the ancient Egyptian civilization body understanding, only 4 previous cases of heart preservation were described in the literature [21, 22]. The heart was positioned by the embalmers on the right side to the vertebral spine after the thoracic cage was emptied of its organs (Figures 5, 6). The heart of Ramses II (XIX Dynasty) was also found to be repositioned on the right side by embalmers [20].
Retroperitoneal organs were not extracted from the body [23], and we found 2 preserved kidneys in true anatomical places (Figure 5). A broken wood stick such as the one that we found in Osirmose's skull has already been found in other mummies skulls, such as the bamboo stick described by Cavka et al [24], and wood fragments described by Wade et al [21]; these sticks may be present due to an accident that occurred during the use of an instrument of natural origin to remove the brain, and dura from the skull (Figure 13). False eyes over the true eye globe were another extrinsic element added to the mummy (Figures 7, 12-14, 16) [13].

Initial visual examination provided the impression that Osirmose's mummy was covered by two layers of bandages: the outer layer placed during a modern restoration and the inner layer blacked with embalming substances. However, 3D CT high-resolution CT showed that the inner layer was the result of a sophisticated embalming procedure with details such as the double layer in the inner layer of the bandage on the right and left side of the oral cavity, and at the level of the oclusal plane on the right and left side (Figures 8, 10, 11).
There was also complex facial and cervical linen stuffing of different anatomical areas such around the ears (Figure 16), in subnasale, supramentale, submaxillary, jugal and in cervical regions (Figures 7, 8, 10, 11, 15)
The mouth was closed (Figures 12, 13, 15) with a piece of linen between anterior teeth (Figure 15). Therefore, the mouth opening ceremony as described by Ruhli et al [25] and occurring in the description of analyses of other mummies, was not used by Osirmose's embalmers. All these details were present and found on 3D CT images because the head of the mummy remained intact until our times (Figures 2-4, 12-14). This also means that artificial holes we found in the maxilla were executed before the death of Osirmose, and are not due to further post-mortem destruction of the mummy (Figures 17, 23). The tooth we found in the oesophagus (Figure 20) may not be in this location due to an accident that occurred during embalming but rather due to a process performed with premeditation, as teeth have already been found in the skull of a mummy from the XXIIth Dynasty [25], in the larynx [25] or between layers of bandages in the back and leg areas [26]. Comparing the difference between the quality of embalming of the face and the traces of the accident during excerebration one might think that embalmers worked in highly specialized teams, and each specific part of the embalming process was in the hands of different specialists [20].
Most advanced bone lesions and wear occurred in the maxilla (Table 1) when

compared to the mandible (Table 2). Egression occurred during the asymmetric wear process (Figures 12, 18, 19, 22). Osteolytic bone lesions were reproduced at successive levels starting from the upper side of the maxilla and continuing to the level of the alveolar bone process (Figure 22). The majority of teeth in the maxilla were lost. Bone lesions were much more aggressive in the maxilla than in the mandible (Table 1, Figures 18, 19). Such asymmetric cases of tooth wear and tooth loss in the upper jaw are present in modern patients with Pica (eating non-nutritive substances) [27], and specifically with geophagia (deliberate eating of earth) [28] when eating argile (kaolinite or clay) [27] or eating seashells [29]. Clay was also reported to be eaten by Ancient Egyptian to treat the gut [28, 30]. The consumption of clay induces iron deficiency, aggressive periodontitis, tooth wear, and asymmetrical tooth loss which is more present in the maxilla than in the mandible [27-29]. Pica or geophagia may be one of the possible explanations for the asymmetric wear process found in Osirmose's mummy.

Table 1. Dental status of maxillary teeth. We applied International Dental Federation teeth numbering.

Teeth present on the dental arch	12, 13, 17, 22, 24, 26 (MV, DV), 27, 28
Teeth missing from the dental arch	11, 14, 15, 16, 18, 21, 23, 25, 26 (P)
Teeth fractured	None
Wear	All present teeth (massive effect on maxillary teeth)
Periapical lesion	12, 13, 17, 18, 22, 26, 27, 28
Recent cavities	26 (vestibular), 27 (vestibular)
Older cavities	17 (vestibular), 17 (palatine), 18 (vestibular), 22 (vestibular), 27 (vestibular), 27 (palatine), 28 (vestibular)
Caries	None
Teeth displaced	25 (oesophagus)
Visible empty socket	16, 23, 25
Abnormal structures	Rectangular hole on the palatine side of tooth n°26 (palatine root of tooth n°26 missing), indentation at right angle palatine to tooth n°27, semi-lunar shape of grooves around the osteolytic lesion distal and palatal to tooth n°28

660 **Table 2.** Dental status of mandibular teeth. We applied the International
661 Dental Federation teeth numbering.

Teeth present on the dental arch	31, 32, 33, 34, 35, 37, 38, 41, 42, 43, 44, 45, 46, 47, 48
Teeth missing from the dental arch	36
Teeth fractured	None
Wear	Yes (all teeth)
Periapical lesion	31, 35 (rarefying osteitis), 46 (rarefying osteitis), 37 (distal root, periodontal disease), 38 (periodontal disease)
Recent cavities	No
Older cavities	31 (vestibular)
Caries	None
Teeth displaced	None
Visible empty socket	None
Abnormal structures	None

662
663 Holes in the maxillary bone in a living person appear by progressive erosion of
664 bone walls starting around the apices of teeth. When the osteolytic bone lesion opens
665 finally through the cortical bone, the tension inside the bone cavity decreases, and
666 the pain for the patient is alleviated. The palatine cortical bone is much more
667 difficult to erode than the vestibular bone because of its thickness. If palatine bone
668 osteolysis occurs, it appears after vestibular bone erosion. For example, we can
669 compare the diameter of vestibular (larger) and palatine (smaller) round openings of
670 bone lesions at the level of the second left molar (n°27) (Figures 21A, 23).
671 Moreover, bone lesion opening initiates at the level of the apex of the root that was
672 infected, as it can be seen in the palatine lesion opening of an infected palatine root
673 of the second left molar (n°27), and of the third left molar (n°28) on the vestibular
674 side (Figure 21A.).
675 The missing bone box that we discovered at the palatine side of the first left molar
676 (n°26) (Figures 17, 23) is situated above a natural localization of the opening of an
677 osteolytic bone lesion, which opens through the bone at the level of the apex of the
678 tooth. Its shape does not correspond to any kind of osteolytic bone lesion described
679 in previous literature [19].
680 Our interpretation is that removal of the palatine root of the first left molar (n°26)
681 was performed in this case with an instrument (possibly metallic pliers), which
682 allowed the removal of the palatine root of the first left molar along with a piece of
683 the palatine cortical plate. The missing bone box therefore corresponds to a
684 "fingerprint" of the use of an oral surgery instrument. At that time, this type of
685 action allowed a large and immediate opening at the thick palatine side of the

infected bone lesion. Palatine root removal was minimally invasive, as two vestibular roots were preserved to allow the patient to continue eating [31]. This means that the notion of dental root anatomy was known, as upper molars have three roots, two vestibular and one palatine. After tooth removal, even in current procedures, a large bone lesion was opened, the inflammatory palatine mucosa was taken out, the pain was gradually decreased, and a local healing process could start. There was also another type of bone opening that was deliberately performed in the same living patient (Figures 17, 23). This time, an operator used a kind of bone curved raspator of approximately 5 mm large, which was long enough to reach the palatine posterior maxilla (Figure 24).

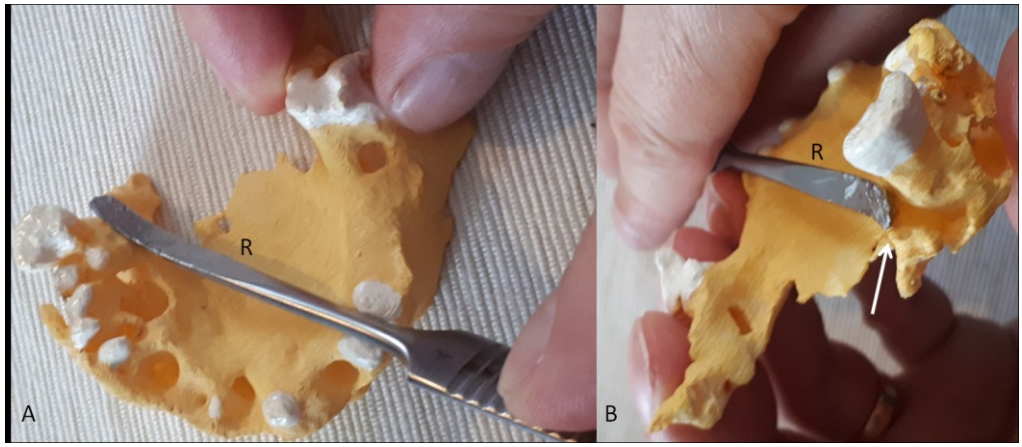

Fig. 24. A. Possible general orientation of the raspator (R) to reach the osteolytic lesion on the palatine side of tooth n°28. B. Posterior view. The raspator (R) placed in the semilunar shaped lesion (arrow) at the palatine side of tooth n°28.

This instrument cut the bone under or through the palatine mucosa and cut the underlying palatine bone corresponding to the floor of the major lesion around and distal to the third left molar (n°28) (Figure 24). Again, the missing bone area corresponds to a "fingerprint" of the instrument used that was left on the bone at the time of oral surgery. This lesion opening was not at a normal level for natural bone lesion openings in this patient, compared to other existing bone lesion openings in the same patient (Figure 21). This action served the same purpose of pain relief and speeding up the healing process of the complex bone osteolytic lesion around the third left molar (n°28). The third element we found was a small step at a right angle in the bone at the level of the palatine side of the palatine root of the second left molar (n°27) (Figures 17, 23). It either belonged to the same instrument and to the same action that was taken to open up the floor of the lesion around the third left molar (n°28), or it was linked to a previous oral surgery attempt in the same area.

Without local anaesthesia, this kind of surgery would be extremely painful therefore, it should only be done as a last choice medical treatment, and as quickly as possible, by a skilled person using adapted instruments.

With this discovery, we hope that other expert teams may start searching for other hidden osseous geometric box holes and semilunar indentations in the maxilla and/or mandible and for "fingerprints" of potential instruments left for eternity in Egyptian museums' mummy collections to further confirm our findings.

- **Acknowledgements**: We would like to thank Mr R. Mazy, the CEO and Professor J.P. Vanoverschelde, medical director of Cliniques universitaires saint Luc, Brussels, Belgium, for allowing us to use the 3D multi-resolution CT scan for non-medical purposes, outside working hours, and without any harm to patients. We would like to thank Mrs Marie-Hélène Grégoire from Presses Universitaires de Louvain for her art work (Figure 1, CC-BY-SA).
- **Funding sources statement**: This study did not receive any funding.
- **Competing interests**: Professor R. Olszewski is Editor-in-Chief of NEMESIS. The all other authors declare no conflicts of interest.
- **Ethical approval**: there was no need for the ethical approval for this study.
- **Informed consent**: there was no need for the informed consent for this study.

Authors contribution:

Author	Contributor role
Olszewski Raphael	Conceptualization, Data curation, Investigation, Methodology, Resources, Validation, Writing original draft preparation, Supervision, Writing review and editing
Hastir Jean-Philippe	Data curation, Resources, Writing original draft preparation, Writing review and editing
Tilleux Caroline	Writing original draft preparation, Writing review and editing
Delvaux Luc	Writing original draft preparation, Writing review and editing

Danse Etienne	Writing original draft preparation, Writing review and editing

References

1. Blomstedt P. Dental surgery in Ancient Egypt. J Hist Dent 2013;61:129-142.

2. Forshaw RJ. The practice of dentistry in ancient Egypt. Br Dent J 2009;206:481-486.

3. Ruffer A. Studies of abnormalities and pathology of ancient Egyptian teeth. Am J Phys Anthropol 1920;3:335-382.

4. Smith GE. Incidence of dental diseases in ancient Egypt. Br Med J 1932;2:760.

5. Hooton EA. Oral surgery in Egypt during the Old Empire. Harvard African Studies 1917;1:29-32.

6. Leek FF. Observations of the dental pathology seen in ancient Egyptian skulls. J Egypt Archaeol 1966;52:59-64.

7. Leek FF. Did a dental profession exist in ancient Egypt during the 3rd millennium B.C.? Med Hist 1972;16:404-406.

8. Melcher AH, Holowka S, Pharoah M, Lewin PK. Non-invasive computed tomography and three-dimensional reconstruction of the dentition of a 2,800-year-old Egyptian mummy exhibiting extensive dental disease. Am J Physical Anthropol 1997;103:329-340.

9. Cesarani F, Martina MC, Ferraris A, Grilletto R, Boano R, Marochetti EF, Donadoni AM, Gandini G. Whole-body three-dimensional multidetector CT of 13 Egyptian humanmummies. Am J Roentgenol 2003;180:597-606.

10. Olszewski R, Tilleux C, Hastir JP, Delvaux L, Danse E. Holding Eternity in One's Hand: First Three-Dimensional Reconstruction and Printing of the Heart from 2700 Years-Old Egyptian Mummy. Anat Rec 2019;302:912-916.

11. Dawson WR. Anastasi, Sallier, and Harris and their papyri. Journal of Egyptian Archaeology 1949;35:158-166.

12. Delvaux L, Therasse I. Sarcophages. Sous les étoiles de Nout. Cercueils et sarcophages des Musées royaux d'Art et d'Histoire. In: Delvaux L, Therasse I, editors. Sarcophages. Sous les étoiles de Nout. Cercueils et sarcophages des Musées royaux d'Art et d'Histoire. 1st ed. Brussels: Racine, 2015.

13 Gray PHK. Artificial eyes in mummies. Journal of Egyptian Archaeology 1971;57:125-126.

14. Taylor JH, Antoine D. Ancient Lives new discoveries. Eight mummies, eight stories. 1st ed. London: British Museum, 2014.

15. Bettum A. Dismutenibtes and Aaiu. Two 25th Dynasty Coffins in Oslo. Studien zur Altägyptischen Kultur 2010;39:51-65.

16. Francot C, Limme L, Van Elst F, Vanlathem MP, Van Rinsveld B. Les Momies égyptiennes des Musées royaux d'Art et d'Histoire à Bruxelles et leur étude radiographique. 1st ed. Turnhout: Brepols, 1999.

17. Maschio F, Pandya M, Olszewski R. Experimental validation of plastic mandible models produced by a "low-cost" 3-Dimensional fused deposition modeling printer. Med Sci Monit 2016; 22:943-957.

18. Olszewski R, Hastir JP, Tilleux C, Delvaux L, Danse E. Computed tomography of the heads of ancient Egyptian mummies: a systematic review of the medical literature. Nemesis 2020;9:1-49.

19. Peluso A. Patologia orale in una antica popolazione egiziana. Dental Cadmos 1980;12:9-28.

20. Brier B. Egyptian Mummies. Unraveling the secrets of an ancient art. Quill Willam Morrow New York, pp 352.

21. Wade AD, Garvin GJ, Hurnanen JH, Williams LL, Lawson B, Nelson AJ, Tampieri D. Scenes from the past: multidetector CT of Egyptian mummies of the Redpath Museum. Radiographics 2012;32:1235-1250.

22 Conlogue G. Considered limitations and possible applications of computed tomography in mummy research. Anat Rec (Hoboken) 2015;298:1088-1098.

23. Salem ME, Eknoyan G. The kidney in ancient Egyptian medicine: where does it stand? Am J Nephrol 1999;19:140-147.

24. Cavka M, Petaros A, Ivanac G, Aganović L, Janković I, Reiter G, Speier P, Nielles-Vallespin S, Brkljacić B. A probable case of Hand-Schueller-Christian's

817 disease in an Egyptian mummy revealed by CT and MR investigation of a dry
818 mummy. Coll Antropol 2012;36:281-286.
819
820 25. Seiler R, Rühli F. "The opening of the mouth"--a new perspective for an ancient
821 827Egyptian mummification procedure. Anat Rec 2015;298:1208-1216.
822
823 26. Scott JW, Horne PD, Hart GD, Savage H. Autopsy of an Egyptian mummy. 3.
824 Gross anatomic and miscellaneous studies. Can Med Assoc J 1977;117:464-469.
825
826 27. Toker H, Ozdemir H, Ozan F, Turgut M, Goze F, Sivas M, Kantarci A. Dramatic
827 oral findings belonging to a pica patient: A case report. International Dental Journal
828 2009;59:26-30.
829
830 28. Macheka LR, Olowoyo JO, Matsela L, Khine AA. Prevalence of geophagia and
831 its contributing factors among pregnant women at Dr. George Mukhari Academic
832 Hospital, Pretoria. Afr Health Sci 2016;16:972–978.
833
834 29. Lavin-Nino de Zepeda S. Pica, a little-known condition in dentistry. Case report.
835 Int J Odontostomat 2019;13:195-197.
836
837 30. Starks PT, Slabach BL. The scoop on eating dirt. Sci Am 2012;306:30-32.
838
839 31. Leek FF. Teeth and bread in ancient Egypt. J Egypt Archaeol 1972;58:126-132.
840
841